Dynamics of Structure and Energy of Horse Carboxymyoglobin after Photodissociation of Carbon Monoxide

Masaaki Sakakura, Shinji Yamaguchi, Noboru Hirota, and Masahide Terazima*

Contribution from the Department of Chemistry, Graduate School of Science, Kyoto University, Kyoto 606, Japan

Received December 21, 1999. Revised Manuscript Received February 26, 2001

Abstract: The energetics and structural volume changes after photodissociation of carboxymyoglobin are quantitatively investigated by laser-induced transient grating (TG) and photoacoustic calorimetric techniques. Various origins of the TG signal are distinguished: the phase grating signals due to temperature change, due to absorption spectrum change, and due to volume change. We found a new kinetics of ∼700 ns (at room temperature), which was not observed by the flash photolysis technique. This kinetics should be attributed to the intermediate between the geminate pair and the fully dissociated state. The enthalpy of an intermediate species is determined to be 61 ± 10 kJ/mol, which is smaller than the expected Fe−CO bond energy. The volume of MbCO slightly contracts (5 ± 3 cm^3/mol) during this process. CO is fully released from the protein by an exponential kinetics from 25 to −2 °C. During this escaping process, the volume expands by 14.7 ± 2 cm^3/mol at room temperature and 14 ± 10 kJ/mol is released, which should represent the protein relaxation and the solvation of the CO (the enthalpy of this final state is 47 ± 10 kJ/mol). A potential barrier between the intermediate and the fully dissociated state is $\Delta H^{\ddagger} = 41.3$ kJ/mol and $\Delta S^{\ddagger} = 13.6$ J mol^{-1} K^{-1}. The TG experiment under a high wavenumber reveals that the volume expansion depends on the temperature from 25 to −2 °C. The volume changes and the energies of the intermediate species are discussed.

1. Introduction

Knowing the relationship between the structural properties of proteins and their reactions is essential for understanding of the protein biological functions. Myoglobin (Mb) has been used as a model system for experimental and theoretical studies of such kinetics−structural relationships. A heme is embedded within the protein, and a small ligand (e.g., O_2, CO, NO) is reversibly bound to the sixth coordination site, on the distal side, of the heme. By photoexcitation of the heme, the ligand−metal bond is photodissociated. Since there is no route prepared to pass the ligand through the protein to the outer solvent, the protein structure has to change if the ligand is removed from the protein. This photoreaction can be used, therefore, to trigger a perturbation to the protein by pulsed laser light.

Extensive research has been conducted to understand the dissociation kinetics and subsequent protein deformation.[1−29] Studies of the reaction kinetics at low temperatures showed that there are several intermediates during the course of the overall

* To whom correspondence should be addressed. Fax: 81-75-753-4000. E-mail: mterazima@kuchem.kyoto-u.ac.jp.

(1) Austin, R. H.; Beeson, K. W.; Eisenstein, L.; Frauenfelder, H.; Gunsalus, I. C.; Marshall, V. P. *Phys. Rev. Lett.* **1974**, *32*, 403.
(2) Hasinoff, B. B. *Biochemistry* **1974**, *13*, 3111.
(3) Austin, R. H.; Beeson, K. W.; Eisenstein, L.; Frauenfelder, H.; Gunsalus, I. C. *Biochemistry* **1975**, *14*, 5355. Takano, T. *J. Mol. Biol.* **1977**, *110*, 569.
(4) Antonini, E.; Brunori, M. *Hemoglobin and Myoglobin and their reactions with ligands*; North-Holland: Amsterdam, 1971.
(5) Austin, R. H.; Chan, S. S. *Biophys. J.* **1978**, *24*, 175.
(6) Case, D. A.; Karplus, M. *J. Mol. Biol.* **1979**, *132*, 343.
(7) Reynolds, A. H.; Rentzepis, P. M. *Biophy. J.*,**1982**, *38*, 15.
(8) Henry, E. R.; Sommer, J. H.; Hofrichter, J.; Eaton, W. A. *J. Mol. Biol.* **1983**, *166*, 443.
(9) Gibson, Q. H.; Olson, J. S.; R. McKinnie, E.; R. Rohlfs, J. *J. Biol. Chem.* **1986**, *261*, 10228. Kuriyan, J.; Wilz, S.; Karplus, M.; Petsko, G. A. *J. Mol. Biol.* **1986**, *192*, 133.
(10) Westrick, J. A.; Goodman, J. L.; Peters, K. S. *Biochemistry* **1987**, *26*, 8313.
(11) Leung, W. P.; Cho, K. C.; Vhau, S. K.; Choy, C. L. *Chem. Phys. Lett.* **1987**, *141*, 220.
(12) (a) Plonka, A.; Kroh, J.; Berlin, Y. A. *Chem. Phys. Lett.* **1988**, *153*, 433. (b) Carver, T. E.; Rohlfs, R. J.; Olson, J. S.; Gibson, Q. H.; Blackmore, R. S.; Springer, B. A.; Sligar, S. G. *J. Biol. Chem.* **1990**, *265*, 20007.
(13) Petrich, J. W.; Poyart, C.; Martin, J. L. *Biochemistry* **1988**, *27*, 4049.
(14) (a) Westrick, J. A.; Peters, K. S. *Biophys. Chem.* **1990**, *37*, 73. (b) Norris, C. L.; Peters, K. S. *Biophys. J.* **1993**, *65*, 1660.
(15) Westrick, J. A.; Peters, K. S.; Ropp, J. D.; Sligar, S.G. *Biochemistry* **1990**, *29*, 6741.
(16) Projahn, H.-D.; Dreher, C.; van Eldik, R. *J. Am. Chem. Soc.* **1990**, *112*, 17.
(17) (a) Spilburg, C. A.; Hoffman, B. M.; Petering, D. H. *J. Biol. Chem.* **1972**, *247*, 4219. (b) Theorell, H. *Biochem. Z.* **1934**, *268*, 73−82. (c) Chatfield, M. D.; Walda, K. N.; Magde, D. *J. Am. Chem. Soc.* **1990**, *112*, 4680.
(18) (a) Srajer, V.; Reinisch, L.; Champion, P. M. *Biochemistry* **1991**, *30*, 4886. (b) Srajer, V.; Reinisch, L.; Champion, P. M. *J. Am. Chem. Soc.* **1988**, *110*, 6656. (c) Steinbach, P. J.; Ansari, A.; Berendzen, J.; Braunstein, D.; Chu, K.; Cowen, B. R.; Ehrenstein, D.; Frauenfelder, H.; Johnson, J. B.; Lamb, D. C.; Luck, S.; Mourant, J. R.; Nienhaus, G. U.; Ormos, P.; Philipp, R.; Xie, A.; Young, R. D. *Biochemistry* **1991**, *30*, 3988. (d) Willis, K. J.; Szabo, A. G.; Krajcarski, D. T. *J. Am. Chem. Soc.* **1991**, *113*, 2000.
(19) Peters, K. S.; Watson, T.; Logan, T. *J. Am. Chem. Soc.* **1992**, *114*, 4276.
(20) Genberg, L.; Bao, Q.; Gracewski, S.; Miller, R. J. D. *Chem. Phys.* **1989**, *131*, 81.
(21) Richard, L.; Genberg, L.; Deak, J.; Chiu, H.-L.; Miller, R. J. D. *Biochemistry* **1992**, *31*, 10703.
(22) (a) Tian, W. D.; Sage, J. T.; Srajer, V.; Champion, P. M. *Phys. Rev. Lett.* **1992**, *68*, 408. (b) Post, F.; Doster, W.; Karvounis, G.; Settles, M. *Biophys. J.* **1993**, *64*, 1833.
(23) Lim, M.; Jackson, T. A.; Anfinrud, P. A. *Proc. Natl. Acad. Sci. U.S.A.* **1993**, *90*, 5801.
(24) Hong, M. K.; Shyamsunder, E.; Austin, R. H.; Gerstman, B. S.; Chan, S. S. *Phys. Rev. Lett.* **1991**, *66*, 2673.
(25) Jackson, T. A.; Lim, M.; Anfinrud, P. A. *Chem. Phys.* **1994**, *180*, 131. Lim, M.; Jackson, T. A.; Anfinrud, P. A. J. *Chem. Phys.* **1995**, *102*, 4355.
(26) Olson, J. S.; Phillips, G. N., Jr. *J. Biol. Chem.* **1996**, *271*, 17593.

10.1021/ja9944655 CCC: $20.00
Published on Web 04/14/2001

process from the ligand−metal bond dissociation to the ligand escape from the protein. However, at ambient temperature in water, the kinetics and the features of the multiple intermediate states have not been elucidated well except for a 180 ns geminate recombination kinetics.[8] Furthermore, although the absorption spectroscopic studies revealed structural changes around the heme chromophore, the structural change in the other part, in particular, the dynamics of the protein structural dynamics, has been less clear. Information regarding the energies of the intermediates is very important, but our knowledge in this respect is very limited, even after the long history of the Mb studies. These difficulties may be solved by using a time-resolved spectroscopy that does not use the optical transition of the heme. The time-resolved photoacoustic calorimetric (PAC) method is one such technique. Peters and co-workers used this method to study the Mb dynamics.[10,11,14,15] From the analysis of the waveforms at various temperatures, the presence of an additional intermediate species was suggested. However, because of inherent limitations of the PAC method as described below, the kinetics is not fully resolved. In this paper, we report a quantitative investigation on the dynamics of the protein of horse heart carboxymyoglobin (MbCO) from 10 ns to milliseconds continuously after photodissociation of CO by a new technique, the laser-induced transient grating (TG) and PAC hybrid method.

Although the volume change (ΔV) and enthalpy change (ΔH)-are very fundamental quantities to characterize in any reaction, it is rather difficult to obtain these quantities experimentally, in particular for irreversible reactions. PAC has been used to measure ΔV and ΔH of many irreversible reactions,[30−32] and it has been also applied to the study of protein dynamics of MbCO previously.[10,11,14,15] A difficulty of the PAC method, however, is that the volume change and enthalpy change contribute to the waveform simultaneously, and they have to be separated. This separation may be accomplished only by measuring the temperature or solvent dependence of the PAC signal. If the volume change or enthalpy change is temperature dependent, the separation of these contributions is impossible. The temperature dependence of the volume change has not yet been examined because of the lack of a proper methodology. Furthermore, if the kinetics is not exponential or there are more than two kinetics in the reaction, the analysis is almost impossible. It is not possible to tell whether the kinetics is exponential from the observed waveform. Another serious difficulty is that the time window of the PAC method is rather limited (10 ns to a few microseconds).

Using the TG signal, these difficulties can be overcome. The time window of the TG method is quite wide, and the temporal development can be directly recorded. We have also demonstrated that ΔV and ΔH can be measured separately without changing the temperature, pressure, or solvent.[33] Later, a TG−PAC hybrid method was proposed to study the energies and structural dynamics of some photochemical reactions.[34,35] Here, we apply this new TG−PAC hybrid method to a biological molecule for the first time in order to analyze the structural and energy dynamics of the MbCO protein after the photodissociation of CO within a time window of 10 ns to a few milliseconds. Miller and co-workers have studied extensively the protein dynamics of MbCO using the TG method in a few nanoseconds time scale[20,21,28] and later extended the observations to a microseconds to milliseconds time range.[29] However, a full analysis of the signal in the long time range has not been performed. We have focused our attention on quantitative investigations in a longer time scale, where the dynamics of the protein's backbone structure becomes important.

2. Experimental Section

The experimental setups for the TG and PAC experiments were reported previously.[33−35] Briefly, the second harmonics of a Nd:YAG laser (Spectra Physics, GCR170) was used for the excitation (pulse width ∼10 ns). A diode laser beam (840 nm) or a He−Ne laser beam (633 nm) was introduced to the crossing region of the excitation beams at an angle to satisfy the Bragg condition. The TG signal was isolated from other scattered light by an interference filter and a pinhole (diameter ∼0.5 mm) and was detected by a photomultiplier (Hamamatsu R928). The repetition rate of the excitation was 3 Hz, which allows the dissociated Mb to return back to the original MbCO.

We used mainly two different regions of the grating wavenumber, q; a relatively low value ($4 \times 10^5-2 \times 10^6$ m^{-1}) and a high value (8.4×10^6 m^{-1}). For the measurement in the low-wavenumber region, the setup is essentially similar to that reported previously.[33,34] The thermal grating signal under this condition decayed with a rate constant of 2−50 μs. For the high-q experiment, the three beams were focused by three separate lenses, and they were crossed at one spot.[35] The crossing angle between two excitation beams was about 50°. Under these conditions, the thermal grating signal decayed very rapidly, with a lifetime of 70 ns. Kinetics slower than this lifetime can be observed clearly without being disturbed by the thermal grating component. The temperature of the sample was controlled by flowing methanol from a thermostatic bath around a metal sample holder and measured with a thermocouple and a voltameter. The fluctuation of the temperature during the measurement was typically smaller than ±0.1 °C. The experiments were repeated several times in different days, and averaged values were calculated.

The second harmonics of a Nd:YAG laser was used for the PAC experiment (spot size ∼0.5 mm diameter). The created pressure wave after photoexcitation was detected by a piezoelectric transducer (a lead zirconate−lead titanate cylinder, Tohoku Kinzoku Co., N-6). The signal was averaged by the digital oscilloscope and transferred to the computer.

Malachite green (MG) in aqueous solution was used as a reference. For the purpose of comparison with previous studies in which deoxymyoglobin (Mb) was used as a calorimetric reference, we confirmed that the TG signal of MG in aqueous solution was the same as that of deoxymyoglobin (Mb) in the Tris buffer solution within our experimental accuracy. Malachite green (Exciton) was used as received.

Myoglobin from horse muscle was purchased from Nakalai Tesque Co. A 50 mM Tris buffer was used. The acidity was adjusted by adding hydrochloric acid to give a pH of 8.0. Small particles or dust in the solution was removed by filtering the solution through a membrane filter. The solution was prepared just before each experiment first by deoxygenation using the nitrogen gas bubbling into the solution for 20 min. Mb was then reduced anaerobically using a slight excess of sodium ditionite, and carbon monoxide was passed over for 20 min to yield

(27) Zhao, X.; Wang, D.; Spiro, T. G. *J. Am. Chem. Soc.* **1998**, *120*, 8517.

(28) Deàk, J.; Chiu, H.-L.; Lewis, C. M.; Miller, R. J. D. *J. Phys. Chem. B* **1998**, *102*, 6621.

(29) Dadusc, G.; Goodno, G. D.; Chiu, H-L.; Ogilvie, J.; Miller, R. J. D. *Isr. J. Chem.* **1998**, *38*, 191.

(30) Simon, J. D.; Peters, K. S. *J. Am. Chem. Soc.* **1983**, *105*, 5156. Bonetti, G.; Vecli, A.; Viappiani, C. *Chem. Phys. Lett.* **1997**, *269*, 268. Hung, R. R.; Grabowski, J. J. *J. Am. Chem. Soc.* **1992**, *114*, 351.

(31) Herman, M. S.; Goodman, J. L. *J. Am. Chem. Soc.* **1989**, *111*, 1849. Herman, M. S.; Goodman, J. L. *J. Am. Chem. Soc.* **1989**, *111*, 9105. Marr, K.; Peters, K. S. *Biochemistry* **1991**, *30*, 1254. Malkin, S.; Churio, M. S.; Shochat, S.; Braslavsky, S. E. *J. Photochem. Photobiol. B* **1994**, *23*, 79.

(32) Schulenberg, P. J.; Braslavsky, S. E. In *Progress in Photothermal and Photoacoustic Science and Technology*; Mandelis, A., Hess, P., Eds.; SPIE: Bellingham, WA, 1997.

(33) Terazima, M.; Hirota, N. J. *Chem. Phys.* **1991**, *95*, 6490. Terazima, M.; Hara, T.; Hirota, N. *Chem. Phys. Lett.* **1995**, *246*, 577. Hara, T.; Hirota, N.; Terazima, M. *J. Phys. Chem.* **1996**, *100*, 10194. Yamaguchi, S.; Hirota, N.; Terazima, M. *Chem. Phys. Lett.* **1998**, *286*, 284.

(34) Terazima, M. *J. Phys. Chem. A* **1998**, *102*, 545−551.

(35) Ukai, A.; Hirota, N.; Terazima, M. *Chem. Phys. Lett.* **2000**, *319*, 427. Ukai, A.; Hirota, N.; Terazima, M. *J. Phys. Chem.* **2000**, *104*, 6681.

the CO form. The stage of ligation of the protein was checked before and after the experiment by measuring the optical absorption spectrum.

3. Analysis

When two laser beams are crossed within the coherence time, an interference (grating) pattern (I_{ex}) is created with a wavenumber q.[36,37] The MbCO sample is photoexcited by this grating light, and the photodissociation reaction is triggered. For an isotropic bulk phase under a weak diffraction condition, the TG intensity (I_{TG}) is proportional to the square of the phase (δn is the phase grating) and/or absorbance (δk is the amplitude grating) differences between the peak-null of the grating pattern.[36]

$$I_{TG} = A(\delta n)^2 + B(\delta k)^2$$

where A and B are constants determined by the experimental conditions. There are several origins for the phase and amplitude gratings. After the optical excitation with a nanosecond laser pulse, one of the dominant contributions is the temperature change of the medium induced by the energy from the radiationless decay of excited states and by the enthalpy change of the reaction. The refractive index change due to this thermal grating, $\delta n_{th}(t)$, is given by

$$\delta n_{th}(t) = (\mathrm{d}n/\mathrm{d}T)/\rho C_p\,[\mathrm{d}Q(t)/\mathrm{d}t * \exp(-D_{th}q^2 t)] \quad (1)$$

where $*$ is the convolution integral, $Q(t)$ is the thermal energy, $\mathrm{d}n/\mathrm{d}T$ is the temperature dependence of the refractive index, ρ is the density, C_p is the heat capacity at a constant pressure, and D_{th} is the thermal diffusivity. When the energy-releasing process can be described by two steps, faster than our response time and a single-exponential process with a lifetime of τ_s, $Q(t)$ is written as

$$Q(t) = Q_f + Q_s[1 - \exp(-t/\tau_s)] \quad (2)$$

where Q_f and Q_s are the thermal energies associated with the fast and slow steps. In this case, $\delta n_{th}(t)$ is written as

$$\delta n_{th}(t) = \{(\mathrm{d}n/\mathrm{d}T)/\rho C_p\}[\{Q_f + Q_s(1 - \tau_s D_{th}q^2)^{-1}\} \times \exp(-D_{th}q^2 t) - Q_s(1 - \tau_s D_{th}q^2)^{-1} \exp(-t/\tau_s)] \quad (3)$$

Another important contribution comes from the change of the absorption spectrum of the solution by photochemical reactions. The newly formed species and the depletion of the original species contribute to the phase and amplitude gratings. We have called this component the population grating. If the molecular volume of the intermediate or the product is different from that of the reactant, the volume change will contribute to the phase grating and is called the volume grating. In this work, "the species grating" is used to describe both of these contributions. (The refractive index change by the species grating (δn_{spe}) is defined by $\delta n_{spe} = \delta n_{pop} + \delta n_{vol}$, where δn_{pop} and δn_{vol} are the refractive changes due to the population and the volume gratings, respectively.)

The species grating signal disappears after the destruction of the spatially periodic pattern of the grating. Any random movement along the grating vector will destroy the signal. When the molecular diffusion is the only source of destruction, the grating pattern disappears with a rate constant of Dq^2 (D is the diffusion constant of the species). When the reactant is regenerated from the product by a back reaction with a time constant k_{back}, the decay of the TG signal is determined by Dq^2 and k_{back}. In the case of MbCO, MbCO is photodissociated to yield Mb and CO, and then Mb and CO recombine to recover MbCO. Three chemical species, MbCO, Mb, and CO, are involved in the species grating. If D of MbCO is similar to that of Mb, the kinetics is written as[38]

$$\delta n_{spe} = \delta n_{co} \exp(-k_{CO}t) + \delta n_2 \exp(-k_{Mb}t) \quad (4)$$

where δn_{co} is the refractive index change induced by the presence of CO and δn_2 is a pre-exponential factor. The decay rate constants are given by

$$k_{CO} = D_{CO}q^2 + k_{back}$$
$$k_{Mb} = D_{Mb}q^2 + k_{back} \quad (5)$$

where D_{CO} and D_{Mb} are the diffusion constants of CO and Mb, respectively. (Since the solution we used was saturated with CO, the recombination kinetics is described by a pseudo-first-order kinetics. This has been confirmed previously in this temperature range (0−20 °C)[3] and also by laser flash photolysis with observation at 633 nm.)

The amplitude grating consists of the periodic grating pattern of a chemical species absorbing the probe light. A mathematical expression similar to eq 4 where δn is replaced by δk gives the temporal profile. The contribution of CO vanishes in this case, because CO possesses no absorption at the probe wavelength.

Here we briefly outline of the separation method. First, the thermal grating signal can be separated from the other contributions by using the characteristic decay rate constant. The thermal grating decays with $D_{th}q^2$, whereas the species grating decays with k_{CO} or k_{Mb}. Second, the amplitude (δk) and phase (δn) gratings can be separated by a signal simulation because the phase grating signal should show an interference effect to δn_{th} or δn_{co} components, which consist of only the phase grating. Third, δn_{pop} always accompanies the absorption change of the sample. Hence, if no absorption change is detected, the observed δn_{spe} should come from δn_{vol}. The volume change can be calculated from δn_{vol} using the relationship

$$\delta n_{vol} = V(\mathrm{d}n/\mathrm{d}V)\Delta N \Delta V \quad (6)$$

where ΔN is the number of the reactive molecules in unit volume, and $V(\mathrm{d}n/\mathrm{d}V)$ is the refractive index change that results from changing the molecular volume. $V(\mathrm{d}n/\mathrm{d}V)$ was obtained from the reported $\mathrm{d}n/\mathrm{d}\rho$ (ρ is the density). Further details will be given in the Results section.

The PAC signal reflects the pressure wave after the photoexcitation, i.e., created by the thermal expansion and the structural volume change. The time profile is written as

$$I_{PA}(t) = \{(\alpha_{th}/\rho C_p)\,\mathrm{d}Q(t)/\mathrm{d}t + \Phi \mathrm{d}\Delta V(t)/\mathrm{d}t\} * g(t) \quad (7)$$

where Φ is the quantum yield of the reaction, α_{th} is the thermal expansion coefficient, ΔV is the structural volume change, and $g(t)$ is the response function of the PAC detector.

4. Results

4.1. TG Signal of MbCO. First we qualitatively describe the features of the TG signal after photoexcitation of MbCO in

(36) Eichler, H. J.; Günter, P.; Pohl, D. W. *Laser induced dynamic gratings*; Springer-Verlag: Berlin, 1986. Fayer, M. D. *Annu. Rev. Phys. Chem.* **1982**, *33*, 63. Miller, R. J. D. In *Time-resolved spectroscopy*; Clark, R. J. H., Hester, R. E., Eds.; John Wiley & Sons: New York, 1989.

(37) Terazima, M. *Adv. Photochem.* **1998**, *24*, 255.

(38) Terazima, M.; Okamoto, K.; Hirota, N. *J. Phys. Chem.* **1993**, *97*, 5188−5192.

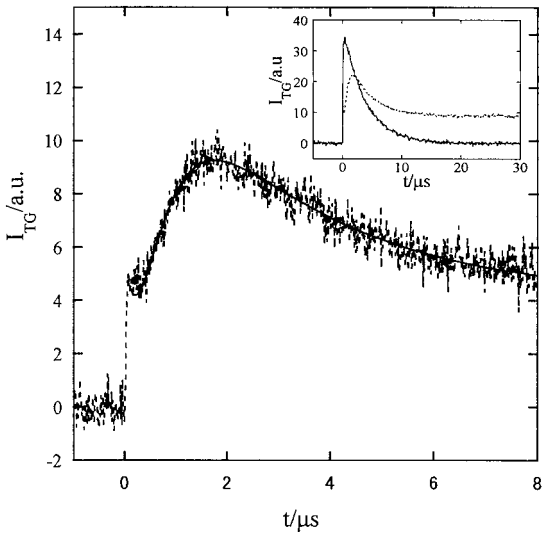

Figure 1. TG signals at 20 °C in a fast time scale after photoexcitation of MbCO in buffer solution (broken line) and the best-fit signal by eq 17 (solid line). The excitation and the probe wavelengths are 532 and 840 nm, respectively. The TG signals from MbCO (broken line) and a reference sample (Malachite green) (solid line) under the same conditions are compared in the inset.

buffer solution from tens of nanoseconds to tens of milliseconds and then quantitatively analyze the signal in the next section. Figure 1 shows the TG signal after the photoexcitation of MbCO in buffer and MG in aqueous solution at 532 nm excitation and 20 °C. The absorbance of MG at 532 nm was the same as that of the MbCO solution. The photophysical process of MG has been completely investigated, and it is well known that all of the photon energy is released to solution much faster than our pulse width.[39] The decay of the TG signal from MG is due to the thermal diffusion, and the rate is given by $2D_{th}q^2$ (eq 1). The MbCO signal rises with a rate determined by the pulse width, and then it decreases a little (not clearly seen at a high temperature such as 20 °C, but it is apparent at lower temperatures, which will be shown later). After the signal decays to a certain intensity, it shows a grow−decay dynamics with a constant background in this time scale. The TG signal of MbCO which decays with a rate similar to that from the reference sample (Figure 1) should be attributed to the thermal grating component. The constant background in this time range should be the species grating signal. The other contributions will be disentangled later.

We found that the species grating signal intensity of the MbCO sample was easily saturated by increasing the excitation laser power, whereas the thermal grating signal was not. This different power dependence is due to a multiphoton excitation during the laser pulse. We measured the TG signal with the lowest laser power to avoid this effect. The square roots of the signal intensities (thermal and species gratings) were linear over the energy range of 0.5−5 μJ/pulse at the excitation spot size.

Figure 2 depicts a long time behavior of the TG signal of MbCO. In this photodissociation reaction, three species, MbCO, Mb, and CO, can contribute to the species grating signal. MbCO and Mb produce both the phase and amplitude gratings. On the other hand, CO contributes only to the phase grating because there is no absorption band at the probe wavelength. The temporal profile of this species grating signal is almost perfectly

(39) Schmidt, G. C. *Ann. Phys.* **1921**, *65*, 247. Ben-Amotz, D.; Harris, C. B. *J. Chem. Phys.* **1987**, *86*, 4856. Ippen, E. P.; Shank, C. V.; Bergman, A.; *Chem. Phys. Lett.* **1976**, *38*, 611. Lian, T.; Locke, B.; Kholodenko, Y.; Hochstrasser, R. M. *J. Phys. Chem.* **1994**, *98*, 11648.

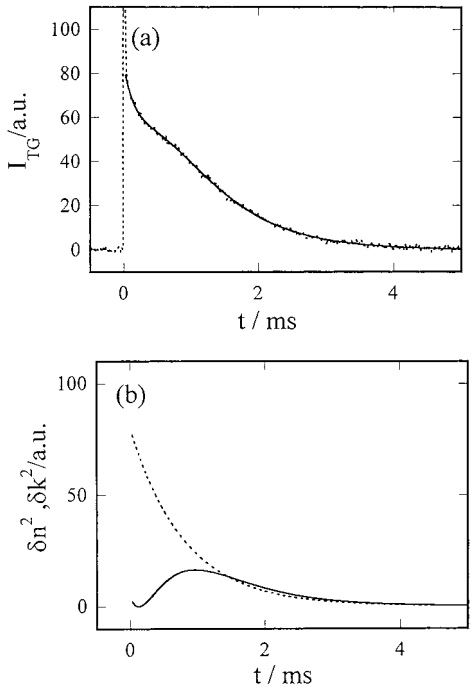

Figure 2. (a) TG signal of MbCO in a long time scale (dotted line). The species grating signal can be separated into phase grating (b, solid line) and amplitude grating (b, dotted line) components. The best-fit signal is shown by the solid line in (a).

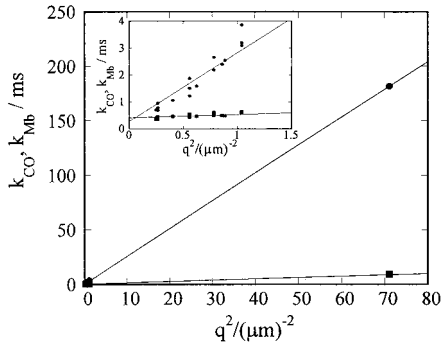

Figure 3. Decay rate constants of the species grating signal k_{CO} (circles) and k_{Mb} (squares) as a function of q^2 (q is the grating wavenumber). The solid lines are the lines fit by eqs 9−11 with the least-squares method. The slopes of the lines represent the diffusion constants of these species, and the intercept indicates k_{Mb}. The inset is the same figure with an expanded scale of the wavenumber axis. The slope is determined mainly by the data set in the low-wavenumber region and that at the high wavenumber ($q = 8.4 \times 10^6$ m^{-1}).

reproduced by eq 4 and the amplitude grating. Using a least-squares fitting, the signal can be separated into δn and δk contributions (Figure 2b), and the decay rate constants, k_{CO} and k_{Mb}, are thus determined. Because the diffusion constant of CO should be much larger than those of Mb or MbCO ($D_{CO} \gg D_{Mb}$), the fast-decaying component is attributed to the species grating due to CO and the slower one to Mb and MbCO ($D_{MbCO} \sim D_{Mb}$). The negative sign of δn_{CO} is consistent with our previous data.[33] From the fitting, we found that the phase grating contribution in the initial part of the signal is almost negligible ($\delta n_{spe} \sim 0$) because of the cancellation between δn_{CO} and δn_2 (eq 4).

Figure 3 shows the plot of the decay rate constants, k_{CO} and k_{Mb}, obtained from the fitting of the species grating signal as a function of q^2. Both rate constants show a good linear relationship against q^2, as expected from eq 5. The intercept of the plot at $\tau = 3$ ms represents the ligand recombination rate (Mb

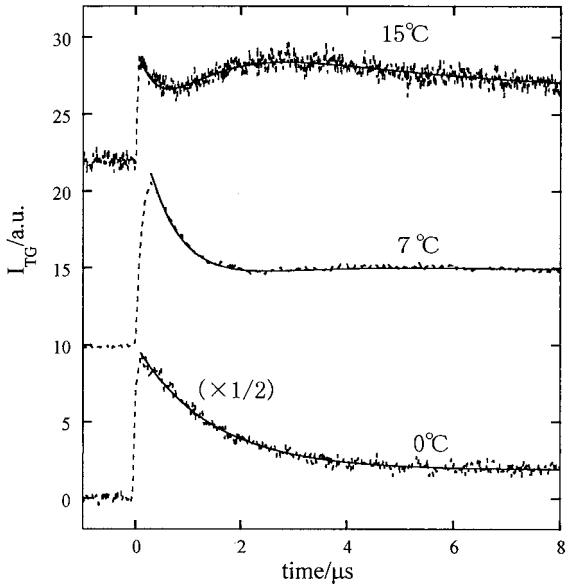

Figure 4. Observed TG signals of MbCO at various temperatures (dotted line): 15.0, 7.0, and 0.0 °C. The best-fit signals by eq 17 are shown by the solid lines.

+ CO → MbCO) and is reasonably close to that measured by the laser flash photolysis experiment probed at 633 nm under the same condition (2.8 ms). The diffusion constants of Mb and CO are determined to be $D_{CO} = (2.6 \pm 0.3) \times 10^{-9}$ m^2 s^{-1} and $D_{Mb} = (1.2 \pm 0.1) \times 10^{-10}$ m^2 s^{-1} from the slope of the plots. D_{CO} from this analysis ($D_{CO} = (2.6 \pm 0.3) \times 10^{-9}$ m^2 s^{-1}) agrees with the previously reported value ($D_{CO} = (3.4 \pm 0.7) \times 10^{-9}$ m^2 s^{-1}).[33] This analysis of the diffusion constant also supports our procedure for the separation of the each species in the species grating signal.

4.2. Energies, Volume Changes, and the Kinetics. The slow rising of the initial part of the TG signal for MbCO (Figure 1) indicates the presence of a slow dynamics in a time scale of 10 ns to 1 μs. To examine the dynamics more clearly, the TG signal of MbCO was measured as a function of temperature in the range of 20 to −2 °C. Some of the signals are depicted in Figure 4. Since $|dn/dT|$ of water decreases with decreasing temperature until $T = 0$ °C, the thermal contribution is expected to become minor at lower temperatures. The species grating signal intensity (background signal in this time scale) remains almost constant with decreasing temperature. This indicates that the quantum yield of the photodissociation of CO is almost temperature independent in this range. On the other hand, the thermal grating signal intensity diminishes at lower temperatures, and another component becomes apparent beneath the thermal grating signal. The decay of this component is well described by a single-exponential function (vide infra). In the rest of this section, these components are identified and quantitatively separated.

A simple interpretation of the fast-decaying component at 0 °C is the population grating associated with the decay of the intermediate species. To investigate the kinetics of the intermediate, we measured the transient absorption signal after the photoexcitation of MbCO. The signal rises within the excitation pulse width and decays with the rate of the CO recombination (2−3 ms). The transient absorption signal intensity detected between 550 and 630 nm is almost constant within the 10 ns to 2 μs range. This observation is consistent with the previous studies showing that the quantum yield of the cage recombination is as low as 4%.[8] Hence, we conclude that the observed kinetics in the TG signal is *not* associated with the absorption change. The population grating component, δn_{pop}, and also the amplitude grating signal, δk_{pop}, should be constant during this time range. We attribute the kinetics in the species grating signal to the molecular volume change; that is, changing the molecular structure forces the solvent molecules to move and consequently causes variations of the refractive index of the solution, leading to the so-called volume grating.[33]

Here we analyze the TG signal in the following way. We describe the volume change by a two-step kinetics, fast and slow (lifetime τ_s),

$$\delta n_{vol}(t) = \delta n_{\Delta V_f} + \delta n_{\Delta V_s}(1 - \exp(-t/\tau_s)) = \delta n_{\Delta V} - \delta n_{\Delta V_s} \exp(-t/\tau_s) \quad (8)$$

where $\delta n_{\Delta V}$ and $\delta n_{\Delta V_{s(f)}}$ are the refractive index changes induced by the total and the slow (fast) volume changes ($\Delta V = \Delta V_f + \Delta V_s$), respectively. The fast volume change takes place within the excitation pulse width, in agreement with previous TG studies.[20,21,28,29] From the analysis of the species grating in the previous section, $\delta n_{spe} = \delta n_{pop} + \delta n_{\Delta V}$ is negligible in this initial time range. Therefore, the time dependence of δn_{spe} is given by

$$\delta n_{spe}(t) = \delta n_{pop}(t) + \delta n_{vol}(t) = -\delta n_{\Delta V_s} \exp(-t/\tau_s) \quad (9)$$

Consequently, the TG signal in this time range should be expressed by

$$I_{TG} = A[\{(dn/dT)/\rho C_p\}\{Q_f + Q_s(1 - \tau_s D_{th} q^2)^{-1}\} \times \exp(-D_{th} q^2 t) - \{\{(dn/dT)/\rho C_p\} Q_s (1 - \tau_s D_{th} q^2)^{-1} \times \delta n_{\Delta V_s}\} \exp(-t/\tau_s)]^2 + B(\delta k)^2 \equiv \{\alpha \exp(-D_{th} q^2 t) - \beta \exp(-t/\tau_s)\}^2 + B(\delta k)^2 \quad (10)$$

The α and β values determined by the least-squares fitting of the signals at various temperatures are plotted in Figure 5a vs dn/dT. At the temperature of $dn/dT = 0$ (i.e., $\delta n_{th} = 0$), the amplitude of the decaying component is given by $\delta n_{\Delta V_s}$. Using the intensity, ΔV_s was determined to be 14.7 ± 2 cm^3/mol (volume expansion) with the reported $\partial n/\partial \rho$ (ρ is the density) of water.[40] If we assume that ΔV_s does not depend on temperature, then the slope of β of Figure 5a gives Q_s, which is −17.4 kJ/mol (*endothermic process*).

We examine the temperature dependence of ΔV_s experimentally by using the TG setup with the high wavenumber. At $q = 8.4 \times 10^6$ m^{-1}, the thermal grating signal decays with a 70 ns lifetime, which is much faster than the volume change (700 ns at 20 °C). Hence, the volume change $\delta n_{\Delta V_s}$ can be directly observed at this high-wavenumber experiment without disturbance from the thermal component. The signal (Figure 6) rises initially fast (<10 ns) and then slowly. The signal then decays with a rate constant of ~700 ns at room temperature. The slow rise represents the decay of the thermal grating signal, which is destructively interfered with by the positive refractive index change of δn_{spe}. From the signal intensity decaying 700 ns (δn_{vol}), we can calculate ΔV_s using the data of $dn/d\rho$ (eq 6). Since the temperature dependence of $dn/d\rho$ is negligible within this temperature range (less than 1%),[40b] the relative signal intensities at various temperatures directly reflect the relative

(40) (a) *Water*; Franks, F.. Ed.; Plenum Press: New York, 1972; Vol. 1. (b) *The structure and properties of water*; Eisenberg, D., Kauzmann, W., Eds.; Oxford University Press: Oxford, 1969.

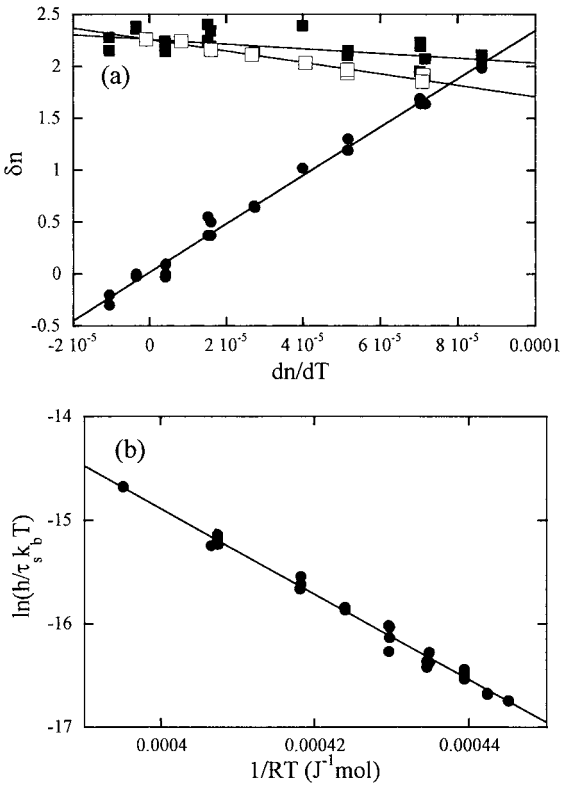

Figure 5. (a) Temperature dependence of α (closed circles), β (closed squares), and $\delta n_{\Delta V_s}$ (open squares) obtained from the fitting of the TG signal with eq 17. The solid lines are least-squares fits of the data with a linear function. (b) Temperature dependence of τ_s obtained from the fitting of the TG signal with eq 17. The solid line is the best-fit line by eq 18.

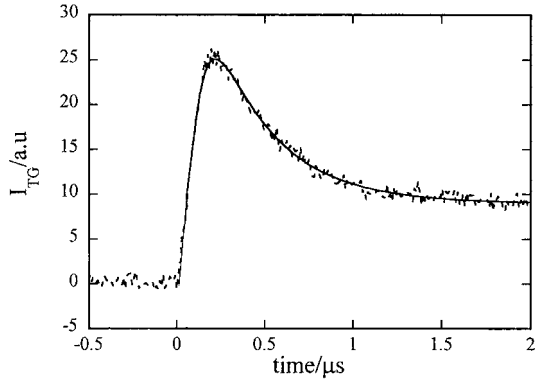

Figure 6. Observed TG signal (broken line) after photoexcitation of MbCO at high grating wavenumber ($q = 8.4 \times 10^6$ m^{-1}) and the best-fit signal (solid line) by eq 17. Note that the signal rise in this case represents the "decay" of the thermal grating signal because $D_{th}q^2$ is much faster than the rate of the volume change.

volume changes at those temperatures. Hence, the observed temperature dependence of the signal intensity indicates that the volume change should depend on the temperature. Although the experimental uncertainty of the absolute value of ΔV is ±2.0 cm^3/mol, which mainly comes from the quantitative comparison of the TG signal intensity of the MbCO sample with that of the reference sample at room temperature, the relative volume change at various temperatures can be measured more accurately (±0.3 cm^3/mol). In all of the previous PAC studies,[10,11,14,15] the volume change was assumed to be temperature independent, as will be discussed in section 5.1. However, we now found that ΔV_s is 14.7 cm^3/mol at room temperature, and, using this value as a standard, it increases to 16.8 ± 0.3 cm^3/mol at 0 °C.

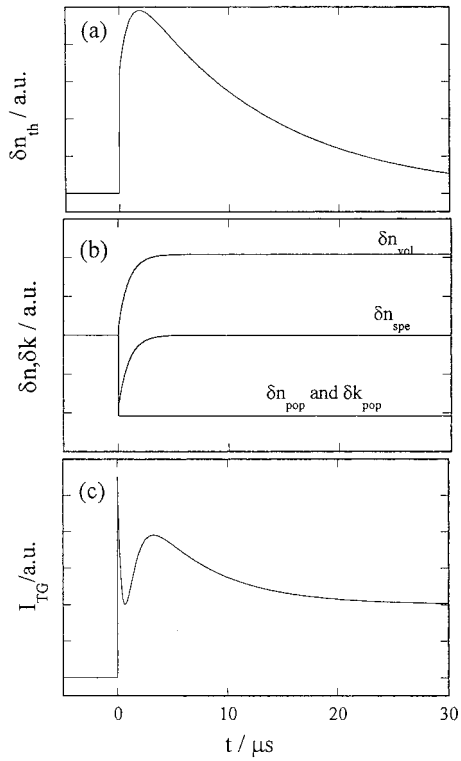

Figure 7. Schematic decomposition of the observed TG signal. (a) Contribution of the thermal grating (δn_{th}), (b) phase population grating (δn_{pop}), amplitude population grating (δk_{pop}), and volume grating (δn_{vol}). The observed TG signal is a square of the total gratings ($A(\delta n_{th} + \delta n_{pop} + \delta n_{vol})^2 + B(\delta k_{pop})^2$).

We calculated Q_s and Q_f from α and β by taking into account the temperature-dependent $\delta n_{\Delta V_s}$ and found that $Q_s = +15$ kJ/mol (*exothermic process*). Using a photon energy of $h\nu = 227$ kJ/mol, we calculate the enthalpies of the first (ΔH_f) and the second (ΔH_s) intermediates as $\Delta H_f = 61 \pm 10$ kJ/mol and $\Delta H_s = 46 \pm 10$ kJ/mol. The observed TG signal can be decomposed into these contributions (δn_{th}, δn_{vol}, δn_{pop}, δk_{pop}) (Figure 7).

Apparently τ_s depends on the temperature (Figure 5b); for example, $\tau_s = 700$ ns at 20 °C and $\tau_s = 2.7$ μs at 0 °C. The activation enthalpy ($\Delta H^{\ddagger}$) and activation entropy ($\Delta S^{\ddagger}$) of the second step are determined from the temperature dependence of τ_s using eq 11,

$$\ln\{h/k_B T\tau_s\} = \Delta S^{\ddagger}/R + (-\Delta H^{\ddagger}/RT) \qquad (11)$$

where k_B is the Boltzmann constant, h the Plank constant, and R the gas constant. The parameters are $\Delta H^{\ddagger} = 41.3$ kJ/mol and $\Delta S^{\ddagger} = 13.6$ J mol^{-1} K^{-1}. Although ΔH_f from the TG measurement and that from the PAC experiments are very different (section 5.1), $\Delta H^{\ddagger}$ and $\Delta S^{\ddagger}$ are close to those reported previously from the PAC method with the two-decays model ($\Delta H^{\ddagger} = 42.6$ kJ/mol and $\Delta S^{\ddagger} = 16.7$ J mol^{-1} K^{-1}).[14a]

The remaining unknown quantity is ΔV_f after the previous simulations. Here we used the PAC method for ΔV_f. The PAC signal from MbCO is fitted by eq 7 with the two kinetics as described above. More accurately than the commonly used approach for the fitting of the PAC signal, the fitting parameter is only ΔV_f in this case (Figure 8). The other parameters are fixed to those determined from the TG analysis. Consequently, we obtained the initial volume change to be $\Delta V_f = -5.2 \pm 3$ cm^3/mol

The energetics and structural dynamics determined in this study are summarized in Figure 9.

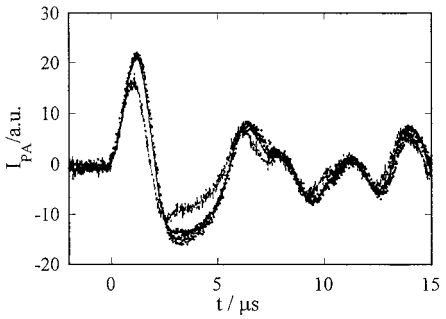

Figure 8. PAC signal of MbCO (dotted line) and the reference (MG) sample at 20 °C (broken line) excited at 532 nm. The best-fit signal of MbCO is shown by the solid line.

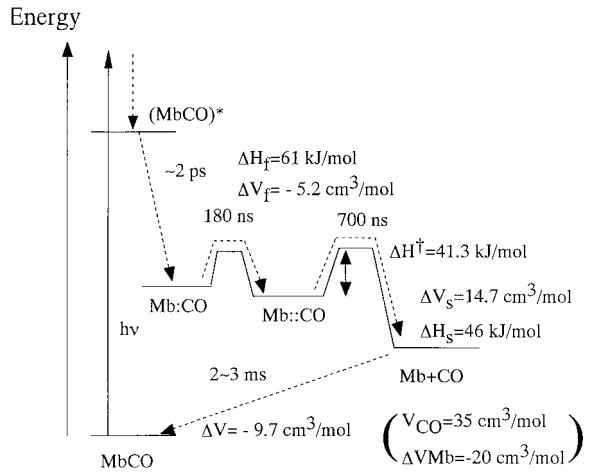

Figure 9. Photodissociation reaction scheme of CO from MbCO. After photoexcitation to the electronic excited state of MbCO, the ligand photodissociates from the heme within 2 ps; the ligand is first trapped in a heme pocket, and from there the CO can recombine to the heme again. With a rate constant of 180 ns, it moves to another trapping site from which it cannot recombine to the heme. This process does not show energetic relaxation or volume change. The ligand escapes from the protein to the solvent in 700 ns at room temperature. The kinetics can be expressed by a single-exponential function. The escaped CO returns to Mb in ~3 ms under this condition.

5. Discussion

5.1. MbCO → Mb::CO. The dissociation and recombination reaction of MbCO is one of the typical model systems and has been studied using various spectroscopies at various temperatures in various solvents.[1−29] After the photodissociation of CO from the iron, the iron atom moves out of the plane of the pyrrole nitrogen atoms very quickly (≤2 ps).[13] To account for the recombination kinetics at low temperatures, three or four intermediates were proposed to intervene between MbCO and fully dissociated Mb.[1,3,9,12,13,16−18,23−27] As a nanosecond kinetics of MbCO, Henry et al. reported a 180 ns decay in the transient absorption signal at 22 °C with 4% geminate recombination quantum yield.[8] The intermediate species is presumably the geminate pair, where the CO is thought to be in the heme pocket (Mb:CO).

The initial structural and enthalpy changes (t < 10 ns) are considered to represent the initial movement of the proximal His and the doming process of the heme plane.[4,8] The 700 ns lifetime at 20 °C observed in the species grating signal is different from the 180 ns kinetics of the geminate pair observed in flash photolysis,[8] suggesting that the intermediate is a species different from the geminate pair. The time-resolved absorbance changes are sensitive only to changes around the chromophore (heme). The 180 ns kinetics probably reflects the diffusion time of the CO out of the heme pocket, which should change the electronic states of the heme. The large structural change (14.7 mL/mol at 20 °C) and enthalpy change in the 700 ns kinetics observed in the TG signal should be interpreted in terms of the escaping process of the CO from the protein to solvent. It is interesting to note that even the Raman scattering and IR absorption due to the heme are not sensitive to this 700 ns process.[24,25] Taking account the two kinetics, we may have the following series of events for the CO dissociation (Figure 9). The CO is trapped in the heme pocket (Mb:CO) after the breaking of the Fe−CO bond. A lifetime of 180 ns corresponds to CO displacement to another trapping site in the protein (Mb:: CO); i.e., CO is located far from the heme. CO then diffuses out with a 700 ns lifetime. This is consistent with the multiple-step scheme proposed for the recombination kinetics at low temperatures.

As an alternative explanation for the observed kinetics, it is also possible that CO diffuses out from the protein with a lifetime of 180 ns, and then a structural relaxation of the protein follows in 700 ns. However, we should remember that the CO-releasing process is a photodissociation reaction: one molecule is split into two molecules, and the volume should increase. It is unlikely that this MbCO dissociation is not associated with the volume change or the enthalpy change. On the other hand, the transfer of the CO out of the heme pocket to another site in the protein matrix would not change the protein structure significantly and could involve only a small change in enthalpy and volume. It is not surprising that the TG signal is not sensitive enough to detect this process.

Peters and co-workers first applied the PAC technique to the photodissociation reaction of MbCO.[10,14,15] Analyzing the PAC waveform at various temperatures and assuming that the volume change and the enthalpy change do not depend on temperature, they found that the intermediate species decays with a lifetime of 850 ns for the sperm whale MbCO and 900 ns for the horse MbCO at 20 °C (taken from the figures in refs 14 and 15). We believe that the kinetics determined from the PAC and from the TG signals represent the same kinetics, because both techniques detect the structural and energy dynamics in common. The slightly different lifetimes may be caused by the fitting uncertainty of the PAC analysis, which involves too many parameters.

Besides the slightly different rates between the PAC and the present study, there is a large difference in ΔH_f (Table 1). ΔH_f = 26 kJ/mol was obtained for the horse MbCO and ΔH_f = 2.5 kJ/mol for the sperm whale MbCO from the PAC analysis. These values are surprisingly smaller than our determined ΔH_f and also smaller than that anticipated for the formation of the geminate pair from a low-temperature kinetic analysis (ΔH_f = 76 kJ/mol).[3] Westrick et al. postulated the breaking of an Arg-45 salt bridge to account for the small ΔH from the PAC measurement.[10,14,15] However, from our results, we do not need to consider the salt bridge breaking to account for ΔH, although this salt bridge breaking could be possible.

We interpret the difference between this work and the previous PAC studies again in terms of the fitting uncertainty of the PAC signal. The error in τ_s could affect the other parameters in the PAC fitting, such as ΔV and ΔH. Another factor we should consider is the temperature change of the volume change. The thermal effect and the volume effect always contribute to the PAC signal simultaneously. The PAC signal was plotted against α_{th}, which should be varied by changing the temperature, and ΔH and ΔV were determined from the

Table 1. Enthalpies (ΔH/kJ mol^{-1}) and Volume Changes (ΔV/cm^3 mol^{-1}) of the Photodissociation of CO and O_2 from Ligated Mb[a]

	buffer	ΔH_f	ΔV_f	ΔH_s	ΔV_s	τ_s	ref
hMbCO[b]	Tris	61 ± 10	-5 ± 3	46 ± 10	14.7 ± 2	700 ns	this work
hMbCO	phosphate	56.3	negative				11
swMbCO	Tris	2.5	−9.2	47.5	5.8	850 ns (20 °C)	15
hMbCO	Tris	31	−1.7	60.5	13.8	900 ns (20 °C)	14a
	phosphate	37	−1.2	60.5	13		
	Tris	26	−1.9	67.2	13	900 ns (20 °C)	14b
swMbCO		84					21
$swMbO_2$	phosphate			73.5			17a
$hMbO_2$	phosphate			63			17a
$hMbO_2$	phosphate			73.5			17b
$swMbO_2$	Tris			22			17c
	phosphate			31			
				180	19.3		16

[a] The subscripts f and s denote the first and second intermediate states, respectively. [b]hMB = horse Mb; swMb = sperm whale Mb.

slope and the intercept at $\alpha_{th} = 0$. In this analysis, the volume change must always be assumed to be temperature independent. Here we found that the temperature dependence of ΔV is not negligible for the Mb system. This temperature-dependent volume change should cause a large errors in ΔH and ΔV from the PAC method.

It is interesting to note that the energy of the first intermediate species determined here (60 kJ/mol) is smaller than the Fe−CO bond enthalpy (105 kJ/mol).[4] This fact indicates that the protein structure is relaxed and stabilized after the CO dissociation within 10 ns. This fast structural relaxation is consistent with the observed volume change in the initial step (−5 cm^3/mol) and also with the observations reported by Miller and co-workers.[20,21,28]

Miller and co-workers extensively investigated the TG signal after the photodissociation of MbCO in a fast time scale and extensively discussed the fast protein movement.[20,21,28] From the quantitative measurement of the thermal grating intensity from MbCO in 75% glycerol/25% water solvent, they determined $\Delta H_f = 84$ kJ/mol.[21] Our ΔH_f (61 kJ/mol) is smaller than this value. However, we recently found that the contribution of the volume change (ΔV_s) cannot be neglected, even in water−glycerol mixture solvent. Furthermore, the protein dynamics in the water−glycerol mixture solvent could be different from that in the buffer solution. These various factors may cause the slight difference and will be re-examined in the future.

We observed a small molecular contraction during the MbCO → Mb:CO process. This change occurs very fast, <10 ns from this study and ~2 ps from the ps-TG experiment.[28] This dynamics probably represents the doming process of the heme plane after the ligand dissociation as well as the relaxation of the protein structure.[4,8]

It is important to point out that the refractive index change around $t = 0$ from our TG analysis is positive,

$$\delta n = \delta n_{th}(t = 0) + \delta n_{pop} + \delta n_{\Delta V_f} > 0$$

which is consistent with the previous report by Richard et al.[21,29] However, contrary to their interpretation, we should note that this positive sign is mainly a result of the positive δn_{pop}, but not of the volume change as suggested previously.[21,29]

5.2. Dissociation of CO from the Protein. After the initial volume contraction associated with MbCO → Mb::CO, a much larger expansion ($\Delta V_s = 14.7$ cm^3/mol at 20 °C) and heating process is observed. This process of the large change may be attributed to the escaping process of CO (Mb::CO → Mb + CO). ΔH of this final dissociated species is obtained to be 46 kJ/mol. On the basis of the enthalpy from the PAC measurements, this Mb::CO → Mb + CO reaction was suggested to be a strongly endothermic reaction. It is difficult to explain the efficiency of CO escaping from the protein. On the other hand, our data indicate an exothermic reaction for this process, and the efficiency of CO escaping from the protein can be explained.

ΔV during the Mb::CO → Mb + CO step is largely positive. However, it should be noted that the molecular volume of the reaction is defined by the sum of the volumes of Mb and CO. The partial molar volume of CO in water has been measured to be 36−37 cm^3/mol, which is larger than ΔV.[33,41] Hence, the protein structure of Mb has to be contracted by ~20 cm^3/mol by releasing the CO to the solvent. This contraction could be related to a change in hydration of the protein, disappearance of the protein cavity, or taking water molecules in the protein structure from the outer solvent. It has been reported that, after the dissociation of the ligand, a water molecule moves closer to the iron atom and is hydrogen-bonded to His-64.[26] It is entirely possible that this movement could affect the molecular volume change.

The temperature-dependent volume change during this process is an interesting phenomenon. The temperature dependence may come from the structural fluctuation of the protein part, which depends on the temperature. However, at present, the origin of the temperature dependence of ΔV is not clear. We are now investigating this new observation by using other protein (mutant Mb) systems. The results will be published elsewhere.

An energy of 14 kJ/mol is released during the escaping process from the protein to solvent. The heat of the transfer of CO from the protein to water was estimated to be about 11 kJ/mol.[11] If this estimation is correct, the energy stabilization of the protein part during the Mb::CO → Mb + CO step is not large but mostly comes from the solvation energy of CO.

We will discuss the kinetics of the volume change finally. In the long history of the Mb studies, nonexponential kinetics have been frequently observed. The nonexponential features in the recombination process of CO at low temperatures have been explained in terms of a broad distribution of the reaction barriers originating from the variety of protein structures. A nonexponential behavior in the geminate recombination was also reported.[22a] These processes have usually been expressed by the stretched exponential function ($\exp(-(kt)^\beta)$ ($0 < \beta < 1$)), and they have been attributed to the structural inhomogeneity of the protein. Hence, it may be interesting to see if there is a nonexponential behavior in the volume change. As described previously, the time-dependent component at 0 °C is represented solely by a single-exponential function 200 ns after the excitation. Also at other temperatures, the kinetics can be fitted

(41) Moore, J. C.; Battino, R. T.; Rettich, R.; Handa, Y. P.; Wilhelm, E. *J. Chem. Eng. Data* **1982**, *27*, 22.

by the single-exponential function. Therefore, we can say that the CO-escaping process does not affect the inhomogeneity of the protein, at least above 0 °C. The exponential kinetics may be due to the fast structural relaxation of the protein at these temperatures.

6. Conclusion

The dynamics of the photodissociation of horse MbCO is investigated by the time-resolved transient grating and photoacoustic calorimetric methods. The TG signal reveals a rich feature from 10 ns to a few milliseconds. After the very fast rise of the signal (<10 ns), the signal decays to a certain intensity and then shows growth-decay in a few tens of microseconds. The later decay in this time range is due to thermal diffusion. The initial state is attributed to a precursor of the fully dissociated state. The other dynamics (700 ns kinetics at 20 °C) is interpreted in terms of the diffusion process of CO from the Mb protein to the solvent. The enthalpy of the initial photodissociation species is 61 kJ/mol, which is smaller than that expected from the Fe−CO bond energy. Therefore, protein structural relaxation takes place in this stage. The volume of MbCO slightly contracts (−5.2 cm^3/mol). During the CO-releasing process, the protein structure is relaxed, and 14 kJ/mol is released. If we assume that the energy of the transfer of CO from the protein to water is 11 kJ/mol,[11] the structural relaxation of the protein part during this process is minor. The volume expands by 14.7 cm^3/mol at 20 °C, and this volume change process is expressed well by a single-exponential kinetics. The Mb protein itself is contracted. Interestingly, the volume change (ΔV_s) depends on temperature. As far as we know, this is the first observation of the temperature-dependent volume change in any irreversible chemical reaction. Two different kinetics, 180 and 700 ns, indicate that there are at least two heme pockets (two potential minima along the dissociation path) before the CO escapes to the solvent. In the hundreds of microseconds to a few milliseconds time range, the dynamics represents the diffusion and recombination reaction of Mb and CO. To fully understand the protein dynamics and the energetics of Mb, quantitative studies of other ligands as well as other Mb (sperm whale and mutants) are now in progress in our group.

Acknowledgment. The authors are indebted to Dr. S. Takahashi, Prof. K. Ishimori, and Prof. I. Morishima of Kyoto University for valuable discussions. A part of this study was supported by a Grant-in-Aid (No.10440173) and the Grant-in-Aid on Priority Area of "Chemical Reaction Dynamics in Condensed Phase" (10206202) from the Ministry of Education, Science, Sports and Culture in Japan.

JA9944655